Pinning and dynamics of colloids on one-dimensional periodic potentials

C. Reichhardt and C. J. Olson Reichhardt
Center for Nonlinear Studies and Theoretical Division, Los Alamos National Laboratory, Los Alamos, New Mexico 87545, USA
(Received 21 September 2004; revised manuscript received 29 March 2005; published 9 September 2005)

Using numerical simulations we study the pinning and dynamics of interacting colloids on periodic one-dimensional substrates. As a function of colloid density, temperature, and substrate strength, we find a variety of pinned and dynamic states including a locked smectic, pinned buckled, two-phase flow, and moving partially ordered structures. We show that for increasing colloid density, peaks in the depinning threshold occur at commensurate states. The scaling of the pinning threshold versus substrate strength changes when the colloids undergo a transition from one-dimensional chains to a buckled configuration.

DOI: 10.1103/PhysRevE.72.032401 PACS number(s): 82.70.Dd

Assemblies of interacting colloidal particles in two dimensions (2D) have attracted considerable attention as an ideal model system in which various types of equilibrium phases can be studied conveniently [1], since the colloid-colloid interactions and density can be changed easily, and the individual colloid positions and motions are directly accessible. When a 1D or 2D periodic substrate is added to the system, new ordering and melting transitions appear. In experiments on colloids interacting with 1D substrates created using interfering laser beams, a novel laser-induced freezing was observed in which the colloids freeze into a crystal as the substrate strength is increased [2]. This effect has also been studied theoretically [3] and numerically [4]. At even higher substrate strengths, a reentrant laser-induced *melting* can occur when the colloids behave one-dimensionally as a line liquid and the fluctuations are effectively enhanced, as predicted initially in theoretical studies [4]. Laser-induced freezing and melting have subsequently been studied both experimentally [5] and theoretically [6–8].

Theoretical studies predicted a rich variety of equilibrium phases, including floating solids, modulated liquids, and locked and floating smectic states, as a function of commensurability between the colloidal crystal and the periodicity of the 1D substrate, which breaks the rotational symmetry of the system [7,8]. The melting was shown, in general, to be reentrant with substrate strength. In the locked smectic phase, described in detail in Ref. [8], the colloids are effectively decoupled between troughs and only short-range order occurs, whereas in the locked floating solid phase, quasi-long-range order exists. In agreement with these predictions, recently experiments showed that the locked floating solid melts into a modulated liquid with intermediate locked smectic phases [9]. The crystalline phases and melting of colloids interacting with 2D periodic substrates have also been studied and a variety of novel equilibrium crystalline orderings and melting phenomena were observed [10–13].

Far less is known about the *dynamical* interactions of colloids with periodic substrates. Recently it was shown that dynamical locking effects can occur for colloids driven over 2D periodic substrates when the colloids preferentially move along the symmetry directions of the substrate [14–17]. Colloids driven over periodic substrates are a useful model system for studying depinning phenomena that also occur in other systems, including vortices in superconductors interacting with periodic pinning arrays [18] as well as atomic friction models [19]. Similar comparisons can be made for colloids driven over random substrates [20].

In this work we consider colloids driven over periodic 1D substrates, which to our knowledge has not been studied previously. We consider parameters relevant to recent experiments on colloids interacting with periodic potentials. For fixed substrate strength and lattice constant, we find that as the colloid density increases, peaks in the depinning threshold occur at various commensurate fillings. In general, we observe a pinned regime, a disordered or plastic flow regime, and partially ordered moving regimes as a function of the driving force. Several types of pinned states appear, including pinned commensurate lattices, pinned or locked smectics, and a buckled phase. For high colloidal densities, where the colloid lattice constant is much smaller along the direction of the substrate minimum, the colloids form a locked smectic state in which all dislocations have Burgers vectors parallel to the substrate, and we show that as the substrate strength decreases there is a change in the scaling of the depinning force versus substrate strength when the colloids undergo a transition from 1D chains to a buckled state.

We simulate a 2D system of N_c colloids with periodic boundary conditions in the x and y directions. The overdamped equation of motion for colloid i is

$$\frac{d\mathbf{r}_i}{dt} = \mathbf{f}_{cc}^i + \mathbf{f}_s + \mathbf{f}_d + \mathbf{f}_T. \tag{1}$$

Here the colloid-colloid interaction force, given by a Yukawa or screened Coulomb potential, is $\mathbf{f}_{cc}^i = -\Sigma_{j\neq i}^{N_c} \nabla_i V(r_{ij})$, where $V(r_{ij}) = (q_i q_j / r)\exp(-\kappa r)$. The colloid charge $q_{i(j)} = 1$, $1/\kappa$ is the screening length, $\mathbf{r}_{i(j)}$ is the position of particle $i(j)$, and $r = |\mathbf{r}_i - \mathbf{r}_j|$. The substrate $\mathbf{f}_s = f_p \sin(2\pi y/d)\hat{\mathbf{y}}$ is periodic in one dimension, as shown in Fig. 1(a), with period d in the y direction. This is the form expected from the modulated laser fields used in the experiments [5]. We measure length in units of d. The external driving force $\mathbf{f}_d = f_d\hat{\mathbf{y}}$ could come from an applied electric field. The thermal force $\mathbf{f}_T$ is a randomly fluctuating force from Langevin kicks. We have considered various system sizes; here we focus on fixed $L_y = 16d$. A triangular colloidal lattice is commensurate with the substrate for $d = \sqrt{3}a/2$, where a is the colloidal lattice con-

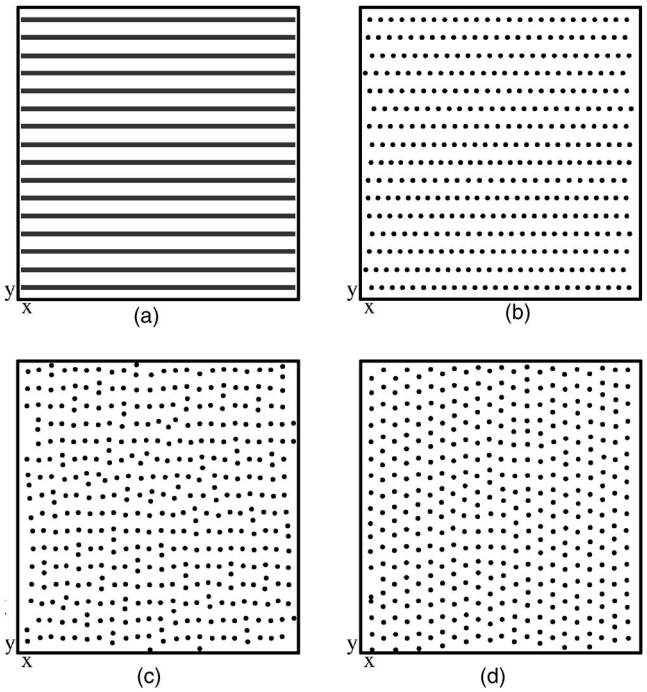

FIG. 1. (a) Heavy lines: locations of the substrate minima. (b)–(d) Black dots: Real space snapshots of the colloid positions for a system with fixed d, $f_p=2.0$, and $n_c=1.35$. (b) Pinned smectic state at $f_d=0$. (c) $f_d/f_c=1.1$, where f_c is the depinning threshold. The colloids are moving in the y direction. (d) $f_d/f_c=1.2$ shows significant triangular ordering.

stant. The density of colloids, n_c, is normalized such that at the commensurate density, $n_c=1.0$. Temperature T is reported in terms of the melting transition T_m for a colloidal lattice at the commensurate density in the absence of the substrate. For the results in this work we focus on the case $T/T_m=0.5$, which is low enough to avoid appreciable creep. The initial colloidal state is obtained at $f_d=0$ by cooling the system from a high-T molten state to lower T. A similar procedure was used to find the equilibrium states for colloids on 2D substrates [10]. The applied drive is then increased from $f_d=0$ by small increments. At each increment, we measure the average colloidal velocity $V_y=\Sigma_{i=1}^{N_c}\mathbf{v}_i\cdot\hat{y}$ after reaching the steady flow state.

We first consider the case of fixed substrate lattice constant d and strength f_p and examine the depinning as a function of colloidal density n_c. In general, we find three regimes: pinned, disordered flow, and a partially ordered high drive flow. We note that for lower pinning forces, additional floating solids or smectic states can occur [7,8], which we do not consider here. The exact type of order in the pinned regime depends on the colloid density. For high densities $n_c>1.0$, the colloidal lattice is anisotropic and at finite T forms a pinned or locked smectic state, as seen in Fig. 1(b) for $n_c=1.35$. The dislocations depin before the particles as the drive is increased so the locked smectic initially depins into a plastic flow or two-phase flow regime, where only a portion of the colloids move. We illustrate this flow in Fig. 1(c), which shows the colloidal positions just above depinning for $f_d/f_c=1.1$, where f_c is the critical depinning force. Here the

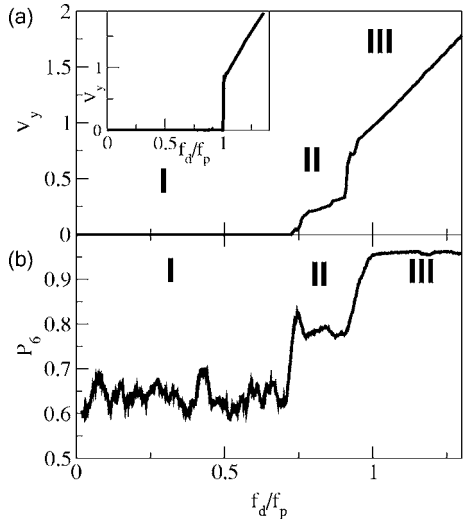

FIG. 2. (a) Average colloidal velocity V_y vs f_d/f_p for the system in Fig. 1 with $f_p=2$ and $n_c=1.35$. Inset: V_y vs f_d/f_p for $n_c=0.375$. (b) The density of six-fold coordinated colloids P_6 vs f_d/f_p for the system in Fig. 1.

colloidal positions are much more disordered. As f_d is further increased, all the colloids depin and form a moving partially ordered state where the colloids regain a considerable amount of triangular ordering, as seen in Fig. 1(d). The colloid lattice also realigns in the direction of the drive. The phases can be identified via the fraction of sixfold coordinated particles $P_6=\Sigma_{i=1}^{N_c}\delta(z_i-6)/N_c$, where the coordination number z_i of each colloid is determined from a Voronoi construction. A locked or floating solid is triangular ($P_6=1.0$) while the smectic phases contain dislocations ($P_6<1.0$).

The different flow regimes and the type of ordering are correlated with characteristics of the colloid velocity versus external force curves. In Fig. 2(a) we plot the average colloid velocity V_y and in Fig. 2(b) we show the corresponding P_6 versus the external drive f_d/f_p for the system with $n_c=1.35$. In Fig. 2(a), there are three regions of the velocity force curve labeled I, II, and III. Region I is a pinned smectic state for $f_d/f_p<0.75$; there are a significant number of dislocations present, so here $P_6=0.65$. The plastic flow region II occurs for $0.75<f_d/f_p<0.95$ and begins when V_y jumps above zero. In the plastic flow regime, V_y is smaller than it would be if all the colloids were moving, and lies below the value that would be obtained by a linear extrapolation of the velocity-force slope at higher drives. A number of the pinned dislocations annihilate in this regime and thus P_6 increases to $P_6=0.78$. For $f_d/f_p>0.94$, there is a final jump in V_y, indicating that more colloids are now moving, and the system enters region III where V_y increases linearly with f_d and all the colloids move with a uniform velocity. Here the colloids form a mostly triangular lattice, giving $P_6=0.95$. In the inset of Fig. 2(a) we show the velocity force characteristics for a system with $n_c=0.375$, where the lattice makes a transition directly from a pinned triangular lattice to a moving triangular lattice. Here the intermediate jumplike features in V_y are missing due to the absence of a plastic flow regime, and $P_6=1.0$ for all f_d. These results indicate that it is the presence of dislocations that give rise to plastic flow.

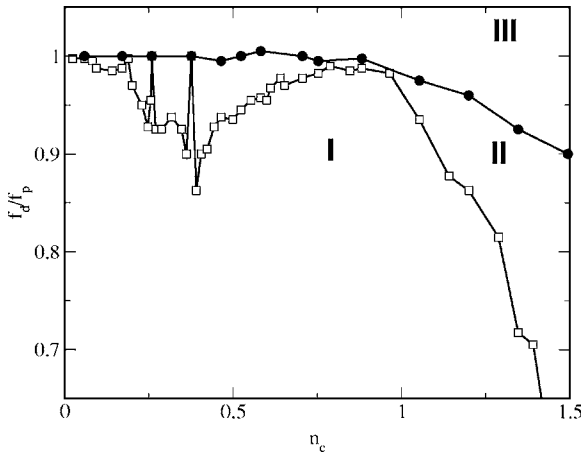

FIG. 3. Flow regions I (pinned), II (plastic), and III (partially ordered) for f_d/f_p vs colloid density n_c at constant $f_p=2.0$. Open squares: depinning threshold. Filled circles: reordering crossover.

In Fig. 3 we map regions I through III as a function of f_d/f_p vs n_c for fixed $f_p=2.0$ and fixed d. The depinning threshold shows several peaks and a prominent broad maximum between $0.75<n_c<1.0$, corresponding to a triangular colloidal lattice. The peaks occur at commensurate densities $n_c=0.38$, 0.26, and 0.185, corresponding to a colloidal lattice constant of $a=\sqrt{2}d$, $\sqrt{3}d$, and $2d$, respectively. At these densities there are no dislocations present in the system and the colloids pass directly from a pinned triangular solid to a moving triangular lattice as a function of driving force without an intermediate disordered flow regime. Region II persists in a small sliver between regions I and III near the commensurability at $n_c=1$ due to the fact that the system was not perfectly commensurate and there were a small number of dislocations present. There is a broad minimum in the depinning threshold centered around $n_c=0.45$. Over this range of density there are significant numbers of dislocations present in the system. For $n_c>1.0$ the depinning threshold drops dramatically with density as dislocations proliferate and the system enters a pinned smectic state. For all densities, once the drive is large enough for all the colloids to depin, the system enters the partially ordered flow regime III. The region III boundary roughly coincides with $f_d=f_p$, although for $n_c>1.0$, the onset of region III shifts slightly down in drive for increasing n_c due to the enhanced colloidal interactions.

The appearance of different dynamic regimes is similar to what is found for vortices driven over 2D random disorder [21,22]. In the vortex case, the plastic flow regime occurs when some vortices are trapped in pinning sites while additional interstitial vortices move between the pins. For strong driving, the vortices can form a moving smectic state aligned with the drive [21] due to transverse barriers. In the 1D periodic pinning case considered here, the partially ordered regime at high drives is a polycrystalline moving solid rather than a moving smectic since there are no transverse barriers.

In experiments with 1D periodic arrays, the substrate strength can be changed by varying the laser intensity. Thus, we consider the effects of altering the substrate force f_p, and find that when the substrate is weakened for $n_c>1.0$, a crossover occurs from the 1D pinned smectic state illustrated in Fig. 1(b) to a buckled configuration. In Fig. 4(a) we plot the critical depinning force f_c vs f_p for a system with fixed $n_c=1.35$. The line in Fig. 4(a) indicates $f_c=f_p$. For $f_p>1.9$ the pinned state is a 1D smectic structure and f_c increases linearly with f_p. For $f_p\leqslant 1.9$, patches of the pinned smectic undergo a buckling transition where the colloids along a single row splay out in a staggered manner, as illustrated in Fig. 4(c) for $f_p=1.0$. The 1D state coexists with the buckled state. Buckled patches do not generally form adjacent to one another due to the increased inter-row colloidal repulsion this would cause. The buckling appears at locations of enhanced stress, where dislocations in the pattern would be present in the 1D pinned case. As f_p is further decreased, the buckled areas grow, as seen in Fig. 4(d) for $f_p=0.75$. For small f_p the colloids form an almost triangular lattice with small distortions, as shown in Fig. 4(e). We note that a different buckling transition has recently been observed in sheared three-dimensional colloidal systems [24].

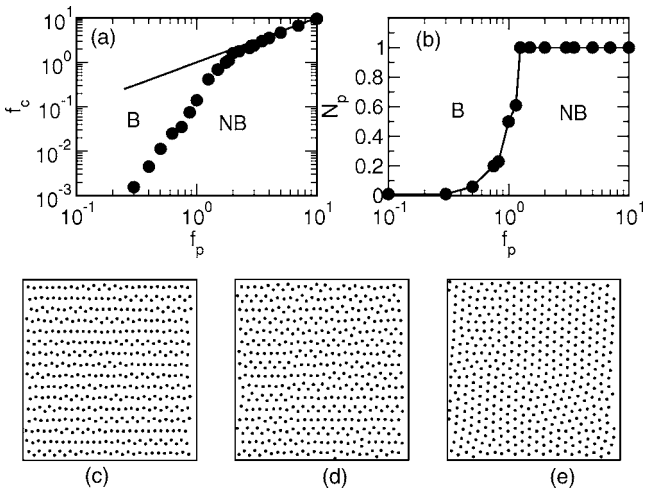

FIG. 4. (a) Squares: critical depinning force f_c vs f_p for fixed $n_c=1.35$. Solid line: $f_c=f_p$ curve. (b) The fraction of colloids N_p in the 1D configuration versus f_p. (c) Buckled state at $f_p=1.0$ and zero drive. (d) Buckled state at $f_p=0.75$ and zero drive. (e) The distorted triangular state at $f_p=0.3$.

The onset of the buckled state coincides with a change from the linear behavior of f_c with f_p to the much more rapid nonlinear decrease for $f_p<1.9$. The linear behavior for large f_p is consistent with single-particle pinning, where the depinning threshold is determined only by the strength of the substrate. The buckled structure is much more weakly pinned than the 1D state since the force acting to push a colloid over the substrate barrier has an additional contribution from the staggered colloids on either side. Collective pinning theory would give $f_c\propto f_p^2$ [23]; however, the decrease we observe appears sharper with a possible $f_c\propto f_p^3$ behavior. For pinning forces at which a buckled pinned state forms, there is both a plastic flow regime and a crossover to region III flow as f_d approaches f_p. In Fig. 4(b) we characterize the onset of the buckling transition via the fraction N_p of colloids that are displaced less than a certain distance in the y direction from the minimum of the potential well. For instance, in Fig. 1(b) all the colloids are in the 1D configuration and sitting at the

bottom of the potential well. In Figs. 4(c) and 4(d), only a portion of the colloids is located at the bottom of the well and for Fig. 4(e) almost no colloids are in the 1D configuration. Figure 4(b) shows that the buckling transition is relatively sharp; however, there is some rounding due to the fact that some dislocations are frozen in the 1D state where the initial buckling occurs.

In conclusion, we have numerically studied the dynamics and pinning of colloids driven over 1D periodic substrates. We find three general regimes: pinned, disordered, and partially ordered, which can be characterized by the amount of disorder in the colloidal lattice and by features in the velocity force curves. We map these regimes as a function of colloid density and show that peaks in the depinning threshold occur at commensurate densities, where triangular or mostly triangular colloid lattices form. As the colloidal density increases for strong substrate strengths, the colloids form a locked smectic state that transforms to a buckled structure as the substrate strength is reduced. In the locked smectic state, the depinning threshold decreases linearly with decreasing substrate strength, while in the buckled state, the depinning threshold decreases much faster than linearly with substrate strength. It would be very interesting to study experimentally both the dynamics of colloids moving over periodic substrates as well as buckling phases for large colloidal densities. Theoretical directions to pursue include examining whether the smectic to buckled phase transition is a true phase transition, and to understand the scaling of the critical depinning versus the substrate strength in the buckled phase.

We thank C. Bechinger and M. B. Hastings for useful discussions. This work was supported by the U.S. DOE under Contract No. W-7405-ENG-36.

[1] C. A. Murray, W. O. Sprenger, and R. A. Wenk, Phys. Rev. B **42**, 688 (1990); K. Zahn, R. Lenke, and G. Maret, Phys. Rev. Lett. **82**, 2721 (1999).
[2] A. Chowdhury, B. J. Ackerson, and N. A. Clark, Phys. Rev. Lett. **55**, 833 (1985).
[3] J. Chakrabarti, H. R. Krishnamurthy, and A. K. Sood, Phys. Rev. Lett. **73**, 2923 (1994).
[4] J. Chakrabarti, H. R. Krishnamurthy, A. K. Sood, and S. Sengupta, Phys. Rev. Lett. **75**, 2232 (1995).
[5] Q.-H. Wei, C. Bechinger, D. Rudhardt, and P. Leiderer, Phys. Rev. Lett. **81**, 2606 (1998).
[6] W. Strepp, S. Sengupta, and P. Nielaba, Phys. Rev. E **66**, 056109 (2002).
[7] E. Frey, D. R. Nelson, and L. Radzihovsky, Phys. Rev. Lett. **83**, 2977 (1999).
[8] L. Radzihovsky, E. Frey, and D. R. Nelson, Phys. Rev. E **63**, 031503 (2001).
[9] J. Baumgartl, M. Brunner, and C. Bechinger, Phys. Rev. Lett. **93**, 168301 (2004).
[10] C. Reichhardt and C. J. Olson, Phys. Rev. Lett. **88**, 248301 (2002).
[11] M. Brunner and C. Bechinger, Phys. Rev. Lett. **88**, 248302 (2002).
[12] K. Mangold, P. Leiderer, and C. Bechinger, Phys. Rev. Lett. **90**, 158302 (2003).
[13] R. Agra, F. van Wijland, and E. Trizac, Phys. Rev. Lett. **93**, 018304 (2004).
[14] P. T. Korda, M. B. Taylor, and D. G. Grier, Phys. Rev. Lett. **89**, 128301 (2002).
[15] M. P. MacDonald, G. C. Spalding, and K. Dholakia, Nature **426**, 421 (2003).
[16] A. Gopinathan and D. G. Grier, Phys. Rev. Lett. **92**, 130602 (2004).
[17] C. Reichhardt and C. J. Olson Reichhardt, Europhys. Lett. **68**, 303 (2004).
[18] M. Baert, V. V. Metlushko, R. Jonckheere, V. V. Moshchalkov, and Y. Bruynseraede, Phys. Rev. Lett. **74**, 3269 (1995).
[19] B. N. J. Persson, *Sliding Friction: Physical Principles and Applications*, 2nd ed. (Springer-Verlag, Heidelberg, 2000).
[20] C. Reichhardt and C. J. Olson, Phys. Rev. Lett. **89**, 078301 (2002).
[21] L. Balents, M. C. Marchetti, and L. Radzihovsky, Phys. Rev. Lett. **78**, 751 (1997); Phys. Rev. B **57**, 7705 (1998).
[22] P. Le Doussal and T. Giamarchi, Phys. Rev. B **57**, 11356 (1998).
[23] A. I. Larkin and Yu. N. Ovchinnikov, J. Low Temp. Phys. **34**, 409 (1979).
[24] I. Cohen, T. G. Mason, and D. A. Weitz, Phys. Rev. Lett. **93**, 046001 (2004).